# Quadratic Scaling of Intrinsic Gilbert Damping with Spin-Orbital Coupling in $L1_0$ FePdPt Films: Experiments and *Ab Initio* Calculations

P. He,[1,4] X. Ma,[2] J. W. Zhang,[4] H. B. Zhao,[2,3] G. Lüpke,[2] Z. Shi,[4] and S. M. Zhou[1,4]

[1]*Surface Physics State Laboratory and Department of Physics, Fudan University, Shanghai 200433, China*
[2]*Department of Applied Science, College of William and Mary, Williamsburg, Virginia 23185, USA*
[3]*Key Laboratory of Micro and Nano Photonic Structures (Ministry of Education) and Department of Optical Science and Engineering, Fudan University, Shanghai 200433, China*
[4]*Shanghai Key Laboratory of Special Artificial Microstructure Materials and Technology and School of Physics Science and Engineering, Tongji University, Shanghai 200092, China*

(Received 26 July 2012; revised manuscript received 10 December 2012; published 12 February 2013)

The dependence of the intrinsic Gilbert damping parameter $\alpha_0$ on the spin-orbital coupling strength $\xi$ is investigated in $L1_0$ ordered $FePd_{1-x}Pt_x$ films by time-resolved magneto-optical Kerr effect measurements and spin-dependent *ab initio* calculations. Continuous tuning of $\alpha_0$ over more than one order of magnitude is realized by changing the Pt/Pd concentration ratio showing that $\alpha_0$ is proportional to $\xi^2$ as changes of other leading parameters are found to be negligible. The perpendicular magnetic anisotropy is shown to have a similar variation trend with $x$. The present results may facilitate the design and fabrication of new magnetic alloys with large perpendicular magnetic anisotropy and tailored damping properties.

DOI: 10.1103/PhysRevLett.110.077203 PACS numbers: 75.78.Jp, 75.30.Gw, 75.50.Vv, 75.70.Tj

Ultrafast spin dynamics in ferromagnets is currently a popular topic due to its importance in magnetic information storage and spintronic applications. The real space trajectory of the magnetization precessional switching triggered by magnetic field pulses, femtosecond laser pulses, or spin-polarized currents [1–6], can be well described by the phenomenological Landau-Lifshitz-Gilbert equation that incorporates the Gilbert damping term describing the dissipation of magnetic energy towards the thermal bath [7]. The magnetic Gilbert damping parameter consists of intrinsic homogeneous and extrinsic inhomogeneous damping terms. The latter is caused by nonlocal spin relaxation processes, leading to Gilbert damping enhancement in thin films and heterostructures and can be tuned by artificial substrates, specially designed buffer and coverage layers [8–10]. For magnetic nanostructures, the extrinsic one caused by the dephasing dynamics is found to strongly depend on the element size [11,12].

The intrinsic Gilbert damping $\alpha_0$ has been thought to arise from combined effects of spin orbital coupling (SOC) and electron-phonon interaction, and has been treated by various theoretical models [13–20]. In the SOC torque-correlation model proposed by Kamberský, contributions of intraband and interband transitions are found to play a dominant role in low and high temperature ($T$) regions, respectively [14,19]. The former (latter) term is predicted to decrease (increase) with increasing $T$ like the conductivity (resistivity) and to be proportional to $\xi^3$ ($\xi^2$). Accordingly, $\alpha_0$ is expected to achieve a minimum at an intermediate $T$. Since the nonmonotonic variation was observed in many $3d$ magnetic metals, the effect of electron-lattice scattering has been well demonstrated [21–23]. In contrast, no direct experiments have been reported to rigorously verify the quantitative relationship between $\alpha_0$ and SOC strength $\xi$ despite many attempts [24–29]. The difficulty lies in the fact that $\alpha_0$ is also strongly related to other physical parameters such as the density of states $D(E_F)$ at the Fermi surface $E_F$ [26,28] and electron scattering time, in addition to $\xi$, and these leading parameters may change when $\xi$ is tailored by using various metals and alloys. More importantly, there is still a lack of an effective approach for continuously tuning the magnetic damping parameter, although the $D(E_F)$ effect has been demonstrated in Heusler alloys and ferromagnetic semiconductors [30–33].

In this Letter, we elucidate the $\xi$ dependence of $\alpha_0$ by using $L1_0$ $FePd_{1-x}Pt_x$(= FePdPt) ternary alloy films with varying Pt/Pd ratio. Time-resolved magneto-optical Kerr effect (TRMOKE) measurements show that $\alpha_0$ can be increased by an order of magnitude when Pd atoms are replaced by Pt because heavier atoms are expected to have a larger $\xi$ [34]. Our calculations show that $\alpha_0$ is proportional to $\xi^2$ at high temperatures because for the present $L1_0$ FePdPt films other parameters are shown to be almost fixed when $\xi$ is artificially modulated by the Pt/Pd concentration ratio. This Letter will provide a clue to continuously alter the magnetic damping and will also facilitate exploration of new magnetic alloys with reasonably high perpendicular magnetic anisotropy (PMA) and low $\alpha$.

A series of $L1_0$ FePdPt ternary alloy films with $0 \leq x \leq 1.0$ were deposited on single crystal MgO (001) substrates by magnetron sputtering. The film thickness was determined by x-ray reflectivity to be $12 \pm 1$ nm. The microstructure analysis was performed by x-ray diffraction. The FePdPt films are of the $L1_0$ ordered structure as proved by the (001) superlattice peak. The chemical ordering degree

 

$S$ can be calculated with the intensity of the (001) and (002) peaks to be about 0.8 for FePt and FePd films. The epitaxial growth was confirmed by a $\Phi$ and $\Psi$ scan with $2\theta$ fixed for the (111) reflection of FePdPt films. In order to measure the Gilbert damping parameter $\alpha$, TRMOKE measurements were performed [35,36]. A variable magnetic field $H$ up to 5 T was applied at an angle of 45° with respect to the film normal using a superconducting magnet. TRMOKE measurements were performed at 200 K in the geometry depicted in Fig. 1(a). Magnetization hysteresis loops were measured by vibrating sample magnetometer at room temperature. The details of fabrication and measurements are described in the Supplemental Material [37].

Figure 1(b) shows the typical TRMOKE results of FePdPt films with various $x$ under $H = 5$ T. The magnetization precession is excited as demonstrated by the oscillatory Kerr signals. Moreover, the magnetic damping is indicated by the decaying precession amplitude with the time delay increasing. In particular, the magnetic damping effect becomes stronger for larger $x$. As shown in Fig. 1(b), the measured Kerr signal can be well fitted by the following equation [35] $\theta_K = a + b\exp(-t/t_0) + A\exp(-t/\tau)\sin(2\pi ft + \varphi)$, where parameters $A$, $\tau$, $f$, and $\varphi$ are the amplitude, magnetic relaxation time, frequency, and phase of the magnetization precession, respectively. Here, $a$, $b$, and $t_0$ correspond to the background signal owing to the slow recovery process. The relaxation time $\tau$ is fitted and found to decrease from about 130.0 to 3.0 (ps) when $x$ changes from 0 to 1.0. Apparently, the magnetic relaxation time can be tuned by the Pt concentration $x$. Figures 1(c)–1(e) display the out-of-plane and in-plane magnetization hysteresis loops for $x = 1.0$, 0.5, and 0.25, respectively. As shown in Fig. 1(c), for $x = 1$ ($L1_0$ FePt) the out-of-plane hysteresis loop is almost square-shaped with coercivity $H_C = 3.8$ kOe, indicating the establishment of high PMA. With decreasing $x$, $H_C$ decreases. For $x = 0.25$ in Fig. 1(e), $H_C$ approaches zero and the out-of-plane and in-plane loops almost overlap with each other, indicating a weak PMA. The PMA therefore increases with increasing $x$ [38]. It is shown that the magnetic relaxation time is strongly correlated with the PMA as a function of the Pt concentration $x$. In experiments, the saturation magnetization for all samples is equal to 1100 emu/cm$^3$ within 10% relative error, close to the bulk value of $L1_0$ FePt [39].

It is essential to uncover the physics behind the $x$ dependence of the magnetic damping effect. Since the extrinsic contribution to $\alpha$ can be suppressed by $H$, the intrinsic one can be extracted by analyzing the TRMOKE results under different $H$ [10,40]. As shown by the TRMOKE results for $x = 0.5$ and 1.0 in Figs. 2(a) and 2(b), the relaxation time becomes shorter with higher $H$ [41], accompanied by a shorter precession period. Figures 2(c) and 2(d) show the $H$ dependencies of the precession frequency $f$ and relaxation time $\tau$ for typical samples. Since the dispersion of the precession frequency with $H$ changes significantly with $x$, the important role of PMA in the precession behavior is clearly demonstrated. It is noted that $\tau$ decreases by two orders of magnitude when Pd atoms are all replaced by Pt ones and reaches about 3.0 ps for $x = 1$ ($L1_0$ FePt). Accordingly, only under high $H$ the magnetization precession can be excited because the oscillation period must be much shorter than the relaxation time [41,42], as shown in Fig. 2(b).

With the magnetic damping parameter $\alpha \ll 1.0$, one can obtain the following dispersion equation $2\pi f = \gamma(H_1H_2)^{1/2}$, where $H_1 = H\cos(\theta_H - \theta) + H_K\cos^2\theta$ and $H_2 = H\cos(\theta_H - \theta) + H_K\cos 2\theta$, $H_K = 2K_U/M_S - 4\pi M_S$ with uniaxial anisotropy constant $K_U$, gyromagnetic

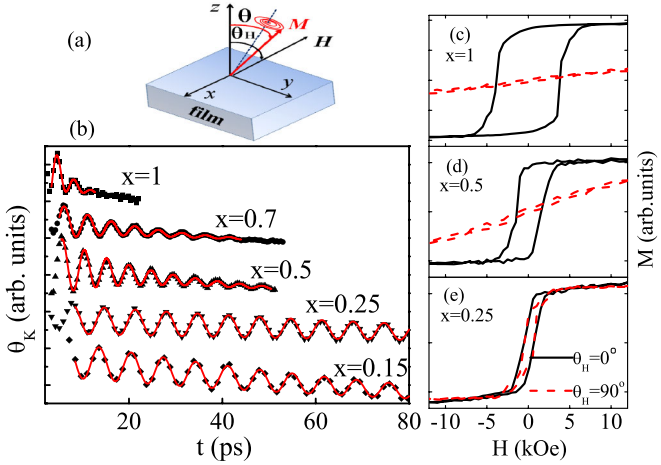


FIG. 1 (color online). Schematic illustration of the TRMOKE geometry (a) and measured TRMOKE results (solid symbols) for $x = 0.15$, 0.25, 0.5, 0.7, and 1.0 with $H = 5$ T and $\theta_H = 45°$ (b). Out-of-plane and in-plane hysteresis loops for $x = 1$ (c), 0.5 (d), and 0.25 (e). In (b) the TRMOKE curves are shifted for clarity and the (red, solid) lines are fit results.

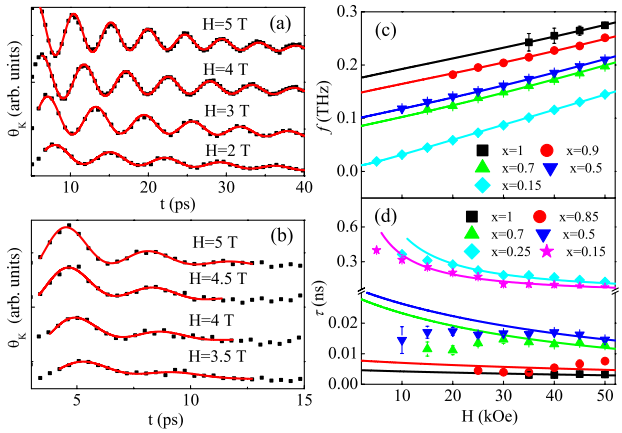


FIG. 2 (color online). TRMOKE results for $x = 0.5$ (a) and 1.0 (b) with various magnetic fields and $\theta_H = 45°$. Uniform magnetization precession frequency $f$ (c) and relaxation time (d) as a function of $H$ for typical samples. In (a) and (b) curves are shifted for clarity. In (a), (b), (c), and (d), solid lines refer to fit results.

ratio $\gamma$, and $\theta_H = 45°$. The equilibrium angular position $\theta$ of the magnetization satisfies the following equation $\sin 2\theta = (2H/H_K)\sin(\theta_H - \theta)$. The measured field dependence of $f$ can be well fitted by the dispersion relation, as shown in Fig. 2(c). With the measured $M_S$ of 1100 emu/cm$^3$, the $g$ factor is calculated and found to increase from 2.03 to 2.16 when $x$ changes from 0 to 1.0. A small fraction of the orbital angular momentum is therefore restored by the SOC, close to other independently reported results [43]. The fitted $K_U$ is shown to increase with increasing $x$, as shown in Fig. 3(a), in agreement with the magnetization hysteresis loops in Figs. 1(c)–1(e). For $\alpha \ll 1.0$, $\alpha$ can be in principle extracted by fitting the measured field dependence of $\tau$ with $\tau = 2/\alpha\gamma(H_1 + H_2)$ and using the fitted values of $g$ and $H_K$. As shown in Fig. 2(d), however, the fits and experimental data coincide at high fields but seriously deviate at low $H$. For continuous magnetic films, inhomogeneous effective anisotropy may contribute to the magnetic damping parameter [8,44]. Since the effect of $H_K$ on the magnetization precession becomes weak with increasing $H$, the extrinsic contribution and thus $\alpha$ should decrease. The extrinsic one is almost suppressed under high $H$ and, accordingly, the fitted $\alpha$ value therefore approximately equals the intrinsic $\alpha_0$ [11,41]. The $\alpha_0$ is found to increase with increasing $x$, as shown in Fig. 3(b).

Spin dependent *ab initio* calculations of the $\xi$ and $\alpha_0$ in $L1_0$ FePdPt films were performed [37]. Here, the intrinsic $\alpha_0$ calculations were concentrated on an interband transition term with a large scattering rate, demonstrating the damping parameter at high temperatures [14,18]. As shown in Fig. 3(b), calculated and measured results of $\alpha_0$ are in good agreement. Calculations show that $\xi$ changes from 0.19 to 0.58 (eV) when $x$ varies from 0 to 1.0, as shown in Fig. 3(c). The $\xi$ is 0.6, 0.20, and 0.06 (eV) for Pt, Pd, and Fe atoms, respectively [34,45], and the effect of Fe atoms is negligible compared with those of Pd and Pt atoms. The present results of $\xi$ are in good agreement with previous *ab initio* calculations [45]. Moreover, the $D(E_F)$ is found to change from 2.55 to 2.39 per atom per eV for $x$ varying from 0 to 1.0. From both x-ray diffraction measurements and theoretical structure analysis of $L1_0$ FePdPt alloys, the lattice constant is found to vary by less than 1.0 percent for different $x$. Standard electron-phonon scattering calculations were performed with the phonon Debye model and static limit of Lindhard's dielectric function. The electron-phonon scattering rate $1/\tau_{e-ph}$ varies from 1.34 to 1.33 ps$^{-1}$ for $x$ changing from 0 to 1.0. Our results show that $1/\tau_{e-ph}$ and $D(E_F)$ are both almost independent of variable $x$. Figure 4 shows that $\alpha_0$ is proportional to $\xi^2$, where the $\xi$ values at other $x$ are interpolated from the fitted curve in Fig. 3(c). Since the lattice constant, $D(E_F)$, Curie temperature, gyromagnetic ratio, electron-phonon scattering rate, and averaged spin, as leading parameters of $\alpha_0$ [19,26,28], are either experimentally or theoretically shown to be almost constant with $x$, the increase of $\alpha_0$ with $x$ is therefore mainly attributed to the larger $\xi$ of Pt atoms. The present Letter has *rigorously* proven the theoretical prediction of the $\xi^2$ scaling of $\alpha_0$ [14], indicating that $\alpha_0$ at high temperatures is mainly caused by interband contribution [14,19]. Moreover, the electronic-scattering-based model of ferromagnetic relaxation is therefore proven to be applicable for $\alpha_0$ in $L1_0$ FePdPt ternary alloys [14]. Further investigation of the magnetization precession at low temperatures will be helpful to get deeper insight into the origin of $\alpha_0$ [19].

The results in Figs. 3(a) and 3(b) are also helpful to address the correlation between $\alpha_0$ and PMA. Up to date, the correlation between these two physical quantities is still unclear although this issue has been studied extensively in theory and experiments [14,15,30–33]. The magnetocrystalline anisotropy is thought to arise from second order energy correction of SOC in the perturbation

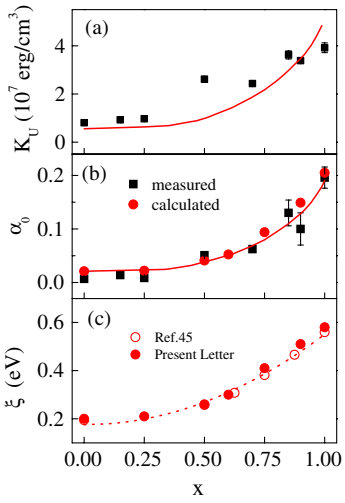


FIG. 3 (color online). Measured $K_U$ (a), measured (solid box) and calculated (solid circle) $\alpha_0$ (b), $\xi$ calculated in this Letter (solid circle) and in Ref. [45] (open circle) (c) as a function of $x$. The line in (c) refers to the polynomial fit results. The fitted lines correspond to proportional functions of $K_U$ (a) and $\alpha_0$ (b) with $\xi^2$ through the fitted results in (c).

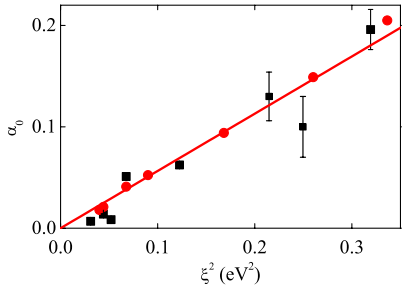


FIG. 4 (color online). Experimental (solid squares) and theoretical (solid circles) values of $\alpha_0$ versus $\xi^2$ obtained for different $x$. The solid curve represents a proportional function fit.

treatment and is roughly proportional to both $\xi$ and orbital angular momentum when $\xi$ is smaller than the exchange splitting. The orbital momentum in $3d$ magnetic alloys restored by SOC is also proportional to $\xi$; therefore, PMA is proportional to $\xi^2/W$ with the bandwidth ($W$) of $3d$ electrons [46]. Since $W$ does not change much with $x$, the enhanced PMA at high $x$ is attributed to a larger $\xi$ of Pt atoms compared with that of Pd atoms [34] and the quadratic scaling law of the PMA with $\xi$ is expected, as proved by the fact that the measured $K_U$ can be fitted by a proportional function of $\xi^2$ in Fig. 3(a). With the same origin in SOC, it can be easily understood that $K_U$ and $\alpha_0$ both show similar variation trends as a function of $x$ when other leading parameters except for $\xi$ are almost fixed with varying $x$ in the $L1_0$ FePdPt alloy films.

In summary, we have investigated the magnetization dynamics in $L1_0$ FePdPt ternary alloy films using TRMOKE. The intrinsic $\alpha_0$ can be continuously tuned, showing an increase with increasing Pt concentration $x$ due to a larger $\xi$ of Pt atoms compared with that of Pd atoms. In particular, the $\xi$ quadratic dependence of $\alpha_0$ has been rigorously demonstrated in experiments. Moreover, $\alpha_0$ and PMA show similar trends with Pt concentration. The present experimental results provide deeper insight into the intrinsic damping mechanism in magnetic metallic materials and provide a new clue to explore ideal ferromagnets with reasonably low $\alpha_0$ and high PMA for applications of magnetic devices.

This work was supported by the MSTC under Grant No. 2009CB929201, (US) DOE Grant No. DE-FG02-04ER46127, NSFC under Grants No. 10974032, No. 11074044, No. 11274240, No. 51171129, No. 51201114, No. 60908005, and No. 61222407, NCET (No. 11-0119), Shanghai PuJiang Program, Grants No. 10PJ004 and No. 10PJ1410300, and Shanghai Committee of Science and Technology under Grants No. 11JC1412700 and No. 10SG26.

[1] L. Landau and E. Lifshitz, Phys. Z. Sowjetunion **8**, 153 (1935); T. L. Gilbert, Phys. Rev. **100**, 1243 (1955).
[2] J. C. Slonczewski, J. Magn. Magn. Mater. **159**, L1 (1996).
[3] Th. Gerrits, H. A. M. van den Berg, J. Hohlfeld, L. Bär, and Th. Rasing, Nature (London) **418**, 509 (2002).
[4] H. W. Schumacher, C. Chappert, R. C. Sousa, P. P. Freitas, and J. Miltat, Phys. Rev. Lett. **90**, 17204 (2003).
[5] S. I. Kiselev, J. C. Sankey, I. N. Krivorotov, N. C. Emley, R. J. Schoelkopf, R. A. Buhrman, and D. C. Ralph, Nature (London) **425**, 380 (2003).
[6] S. Kaka, M. R. Pufall, W. H. Rippard, T. J. Silva, S. E. Russek, and J. A. Katine, Nature (London) **437**, 389 (2005).
[7] B. Koopmans, J. J. M. Ruigrok, F. Dalla Longa, and W. J. M. de Jonge, Phys. Rev. Lett. **95**, 267207 (2005).
[8] R. Urban, G. Woltersdorf, and B. Heinrich, Phys. Rev. Lett. **87**, 217204 (2001).
[9] D. J. Twisselmann and R. D. McMichael, J. Appl. Phys. **93**, 6903 (2003).
[10] G. Woltersdorf, M. Buess, B. Heinrich, and C. H. Back, Phys. Rev. Lett. **95**, 037401 (2005).
[11] A. Barman, S. Wang, J. Maas, A. R. Hawkins, S. Kwon, J. Bokor, A. Liddle, and H. Schmidt, Appl. Phys. Lett. **90**, 202504 (2007).
[12] A. Laraoui, J. Vénuat, V. Halté, M. Albrecht, E. Beaurepaire, and J.-Y. Bigot, J. Appl. Phys. **101**, 09C105 (2007).
[13] B. Heinrich, D. Fraitová, and V. Kamberský, Phys. Status Solidi **23**, 501 (1967).
[14] V. Kamberský, Czech. J. Phys. **26**, 1366 (1976); V. Kamberský, Phys. Rev. B **76**, 134416 (2007).
[15] D. Steiauf and M. Fähnle, Phys. Rev. B **72**, 064450 (2005).
[16] A. Brataas, Y. Tserkovnyak, and G. E. W. Bauer, Phys. Rev. Lett. **101**, 037207 (2008).
[17] M. C. Hickey and J. S. Moodera, Phys. Rev. Lett. **102**, 137601 (2009).
[18] K. Gilmore, Y. U. Idzerda, and M. D. Stiles, Phys. Rev. Lett. **99**, 027204 (2007).
[19] K. Gilmore, Y. U. Idzerda, and M. D. Stiles, J. Appl. Phys. **103**, 07D303 (2008).
[20] H. Ebert, S. Mankovsky, D. Ködderitzsch, and P. J. Kelly, Phys. Rev. Lett. **107**, 066603 (2011).
[21] B. Heinrich and Z. Frait, Phys. Status Solidi **16**, K11 (1966).
[22] S. M. Bhagat and P. Lubitz, Phys. Rev. B **10**, 179 (1974).
[23] B. Heinrich, D. J. Meredith, and J. F. Cochran, J. Appl. Phys. **50**, 7726 (1979).
[24] S. Ingvarssona, G. Xiao, S. S. P. Parkin, and R. H. Koch, Appl. Phys. Lett. **85**, 4995 (2004).
[25] C. Scheck, L. Cheng, I. Barsukov, Z. Frait, and W. E. Bailey, Phys. Rev. Lett. **98**, 117601 (2007).
[26] J. O. Rantschler, R. D. McMichael, A. Castillo, A. J. Shapiro, W. F. Egelhoff, B. B. Maranville, D. Pulugurtha, A. P. Chen, and L. M. Connors, J. Appl. Phys. **101**, 033911 (2007).
[27] G. Woltersdorf, M. Kiessling, G. Meyer, J.-U. Thiele, and C. H. Back, Phys. Rev. Lett. **102**, 257602 (2009).
[28] A. A. Starikov, P. J. Kelly, A. Brataas, Y. Tserkovnyak, and G. E. W. Bauer, Phys. Rev. Lett. **105**, 236601 (2010).
[29] A. Rebei and J. Hohlfeld, Phys. Rev. Lett. **97**, 117601 (2006).
[30] S. Mizukami, E. P. Sajitha, D. Watanabe, F. Wu, T. Miyazaki, H. Naganuma, M. Oogane, and Y. Ando, Appl. Phys. Lett. **96**, 152502 (2010).
[31] S. Mizukami, F. Wu, A. Sakuma, J. Walowski *et al.*, Phys. Rev. Lett. **106**, 117201 (2011); S. Mizukami, S. Iihama, N. Inami, T. Hiratsuka, G. Kim, H. Naganuma, M. Oogane, and Y. Ando, Appl. Phys. Lett. **98**, 052501 (2011).
[32] A. Barman, S. Wang, O. Hellwig, A. Berger, E. E. Fullerton, and H. Schmidt, J. Appl. Phys. **101**, 09D102 (2007).
[33] S. Pal, B. Rana, O. Hellwig, T. Thomson, and A. Barman, Appl. Phys. Lett. **98**, 082501 (2011).
[34] K. M. Seemann, Y. Mokrousov, A. Aziz, J. Miguel *et al.*, Phys. Rev. Lett. **104**, 076402 (2010).
[35] W. K. Hiebert, A. Stankiewicz, and M. R. Freeman, Phys. Rev. Lett. **79**, 1134 (1997).

[36] M. van Kampen, C. Jozsa, J. T. Kohlhepp, P. LeClair, L. Lagae, W. de Jonge, and B. Koopmans, Phys. Rev. Lett. **88**, 227201 (2002).
[37] See Supplemental Material at http://link.aps.org/supplemental/10.1103/PhysRevLett.110.077203 for details of sample fabrications, microstructure characterization, TRMOKE measurements, and *ab initio* calculations.
[38] S. Jeong, A. G. Roy, D. E. Laughlin, and M. E. McHenry, J. Appl. Phys. **91**, 8813 (2002).
[39] O. A. Ivanov, L. V. Solina, V. A. Demshina, and L. M. Magat, Fiz. Met. Metalloved. **35**, 92 (1973).
[40] Z. Celinski and B. Heinrich, J. Appl. Phys. **70**, 5935 (1991).
[41] J. W. Kim, H. S. Song, J. W. Jeong, K. D. Lee, J.-W. Sohn, T. Shima, and S.-C. Shin, Appl. Phys. Lett. **98**, 092509 (2011).
[42] Z. Z. Zhang, B. Cui, G. Wang, B. Ma, Q. Y. Jin, and Y. Liu, Appl. Phys. Lett. **97**, 172508 (2010).
[43] I. V. Solovyev, P. H. Dederichs, and I. Mertig, Phys. Rev. B **52**, 13419 (1995).
[44] Y. Tserkovnyak, A. Brataas, and G. E. W. Bauer, Phys. Rev. Lett. **88**, 117601 (2002).
[45] P. He, L. Ma, Z. Shi, G. Y. Guo, J.-G. Zheng, Y. Xin, and S. M. Zhou, Phys. Rev. Lett. **109**, 066402 (2012).
[46] P. Bruno, Phys. Rev. B **39**, 865 (1989).